THE FULL WAVEFORM ACOUSTIC LOG INVERSION PROBLEM

by

G.H. Garcia and C.H. Cheng

Earth Resources Laboratory
Department of Earth, Atmospheric, and Planetary Sciences
Massachusetts Institute of Technology
Cambridge, MA 02139

ABSTRACT

This paper presents the full waveform acoustic log inversion problem for a multisource - multireceiver tool logging a cylindrical fluid-filled borehole. The problem is formulated in the frequency-depth domain. A priori knowledge about the source array spectra and the borehole formation parameters (velocity, attenuation, density) is taken into account. It is shown that the inversion problem can be formulated as a Separable Nonlinear Least Squares (SNLS) problem with separable nonlinear equality constraints. The case where the source is known and parameterized is studied with synthetic data and an inversion for V_p, V_s, V_f, and ρ_b is implemented and studied.

INTRODUCTION

Full waveform acoustic logging has become a widely used tool in formation evaluation. However, up to now the techniques for determination of formation compressional and shear wave velocities and formation attenuation have been done separately. In "slow" formations shear wave velocities cannot be determined directly and have to be inverted from Stoneley wave velocities. In some tools, the source-receiver characteristics prevent one from identifying the Stoneley wave in "slow" formations. Measurements of formation attenuation are complicated by the effects of modal dispersion. The obvious answer to all these problems is the simultaneous determination of the formation velocity, attenuation, and density from inversion of the full waveform data using a model of elastic wave propagation in a borehole. In this paper, we address the full waveform inversion problem from a theoretical point of view of a constrained least squares inversion. We introduce the concept of separable least squares to decouple the effects of the source from the responses of the formation. We then present some results from the inversion of synthetic full waveform acoutic logging data and study the sensitivity of the waveform to the variations in each individual parameter.

INVERSION THEORY

Statisticians usually distinguish two broad kinds of data analysis problems (Parzen, 1978):

(1) "Statistical Inference-type 1" or model analysis:

Problem: What is the answer to a mathematically well-posed question?

Approach: Theorems on the properties of algorithms derived from estimation and optimization theory.

(2) "Statistical Inference-type 2" or model synthesis:

Problem: What is the question, or equivalently what is the model?

Approach: Data analysis procedures to be learned by doing (observations, experimentation, modelling...)

This paper deals with a "statistical inference-type 1" problem, the full waveform acoustic inversion in a cylindrical borehole geometry. This is a parametric inversion method as opposed to non-parametric inversion methods such as semblance or correlation.

Previous work in parametric and non-parametric inversion

Parametric modelling is common practice in many applications, the very general Autoregressive Moving Average (ARMA) formulation for time series being one of the better known examples. In ARMA modelling, the spectrum of the process is parameterized by a rational fraction in the frequency domain.

For the cylindrical full waveform inversion problem, one considers a parametric form of the frequency-wavenumber spectrum with a finite number of parameters. Much is lost in the inference process if the parametric form is ignored, because when the number of parameters is small compared with the total number of observations, the results of the inference will be much stronger than when using a non-parametric approach. Parametric methods involve statements about the probability distribution of the observed data. Parametric inference presupposes a known form of the statistical distribution of the data being inverted for. Because of the finite amount of data, the class of probability distribution is relatively restricted, usually to the exponential family including Poisson, Gaussian, Binomial, etc., via the probability distribution. The model is above all a mathematical formulation of the knowledge about the tool-borehole-formation system under study. Equation (1), for example, reflects an hypothetical link between the observed signal and the unknown signal. In other words, there exists an expected value of the borehole wavefield signal in the form of a model-hypothesis built from physical laws (the wave equation in cylindrical geometry).

By comparison, the non-parametric approaches, such as semblance or correlation methods, do not make any assumption about the statistical distribution of the data. For the determination of P- and S-wave velocities for instance, most of the work has concentrated so far on non-parametric inversion methods (Willis, 1983; Willis and Toksöz, 1982). Non-parametric methods are usually more expedient and robust (i.e., results are practically independent of any statistical distribution of the data) than their parametric counterpart. Recent asymptotic optimality results, however, show that these methods cannot be substantially improved without the more stringent modelling assumptions (Yakowitz, 1985). They are used in situations where other estimators are difficult to implement because of mathematical manipulative difficulties. They often rely, however, on heuristic techniques such as windowing, threshold detection, etc.

Moreover, in slow formations, where the shear wave velocity is lower than the borehole fluid velocity, non-parametric semblance/correlation methods cannot extract the shear wave information -- although present -- directly from the data. In these cases, one is justified in trying the more "fragile" and compute-intensive parametric inversion methods by using models of the tool-borehole system with additional a priori knowledge in the form of constraints.

In this paper, the forward model structure assumed is set forth and the method of Maximum Likelihood (ML), one of the most versatile and powerful tools of estimation, will be used for inference on the parameters and the associated estimation error covariance.

When there is a priori knowledge on the parameters (for example, data from a density tool, a Caliper Log, or an initial inverse from a non-parametric method), the Maximum A Posteriori (MAP) method will provide (via the Bayes theorem) a way to systematically incorporate these a priori in the inversion.

Since the source function is in general not known, this will then lead to the Constrained Separable inversion method which eliminates the source function inversion from the formation parameters inversion proper and allows a priori about the source and the formation parameters to be taken into account.

THE CYLINDRICAL FORWARD MODEL ASSUMPTIONS

The assumptions are illustrated in Figure 1. The pressure frequency response $P(r,z,\omega)$ in a fluid filled borehole at an axial distance z and radial distance r from a point isotropic source is well known (Tsang and Rader, 1979; Cheng et al., 1982). It is given by

$$P(\omega,z,\Theta) = \left[\frac{\pi e^{-i\frac{\omega}{\alpha_f}\sqrt{r^2+z^2}}}{\sqrt{r^2+z^2}} + \int_{-\infty}^{+\infty} A(\Theta_\alpha) I_0(fr)\, e^{ikz}\, dk \right] X(\omega) \qquad (1)$$

where $X(\omega)$ is the complex Fourier spectrum of the source. The first term within the brackets represents the direct source term. $A(\Theta_\alpha)$, the modal coefficient, is given by

$$A(\Theta_\alpha) = \frac{g(\Theta_\alpha)K_1(fR) - K_0(fR)}{g(\Theta_\alpha)I_1(fR) + I_0(fR)} \qquad (2)$$

and

$$g(\Theta_\alpha) = \frac{f\rho}{l\rho_b}\left\{ \left(\frac{2V_s^2}{c^2} - 1\right)^2 \frac{K_0(lR)}{K_1(lR)} - \frac{2V_s^2 lm}{\omega^2}\left[\frac{1}{mR} + \frac{2V_s^2}{c^2}\frac{K_0(mR)}{K_1(mR)} \right] \right\} \qquad (3)$$

where Θ_α is the parameter vector:

$$\Theta_a = (V_p, V_s, V_f, Q_p, Q_s, Q_f, \rho_b, \rho_f, R)^T \quad (4)$$

and

$$l = k(1-\frac{c^2}{V_p^2})^{1/2} = \omega(\frac{1}{c^2}-\frac{1}{V_p^2})^{1/2} \ ;$$

$$m = k(1-\frac{c^2}{V_s^2})^{1/2} = \omega(\frac{1}{c^2}-\frac{1}{V_s^2})^{1/2} \ ;$$

$$f = k(1-\frac{c^2}{V_f^2})^{1/2} = \omega(\frac{1}{c^2}-\frac{1}{V_f^2})^{1/2} \ ;$$

ω is the angular frequency; c is the phase velocity; $k = \omega/c$ is the axial wave number; V_p ,V_s and V_f are the P and S wave velocity of the formation and the borehole fluid velocity; respectively; R is the borehole radius; ρ_b and ρ_f are the formation and fluid density; and I_i and K_i are the modified Bessel functions of the i^{th} order. The term $A(\Theta_a)I_0(f\tau)$ represents the response of the borehole.

Formation and fluid attenuations appear as the imaginary parts in the complex velocities V_p ,V_s, V_f (Cheng et al., 1982).

THE DISCRETE FORWARD CYLINDRICAL MODEL

The one source, one receiver (1S-1R) tool

For one source and one receiver separated by a distance z, equation (1) above can be written:

$$P(\omega,z,\Theta) = G(\omega,z,\Theta)\ X(\omega) \quad (5)$$

The observed waveform W at frequency ω is modelled as:

$$W(\omega) = G(\omega,z)\ X(\omega) + N_z(\omega) \quad (6)$$

where $W(\omega)$ is the Fourier transform of the observed output field, $P(\omega,z,\Theta)$ is the modelled output pressure field, $X(\omega)$ is the input source and $N_z(\omega)$ is the corrupting observation noise.

$G(\omega, z, \Theta)$ is the complex frequency response of the tool-borehole formation system at frequency ω. It represents the term within brackets in Equation (1). Θ is a parameter vector, a subset of Θ_a shown in Equation (4). One or more of the parameters in Θ_a may be fixed or known a priori with some uncertainty. The source function may also be parameterized by a vector ξ

$$X(\omega) = X(\omega,\xi)$$

and ξ may be included in the inversion.

The Fourier spectrum of the pressure can be discretized at N_ω frequencies $\{\omega_i\}, i=1,N_\omega$, as follows: (This is a valid approximation by the Stone-Weirstrass theorem if the power spectral density matrix of the modelled process is positive definite and continuous)

$$P(\omega_i,z,\Theta) = G(\omega_i,z,\Theta)\ X(\omega_i) \qquad \{i=1,...,N_\omega\}$$

In matrix form the N_ω equations above become:

$$\mathbf{P}(z,\Theta) = \mathbf{G}(z,\Theta)\ \mathbf{X} \tag{7.a}$$

where:

$$\mathbf{P}(z,\Theta) = \{P(\omega_i,z,\Theta),\ i=1,\cdots N_\omega\} \tag{7.b}$$

$$\mathbf{G}(z,\Theta) = Diag\{(G(\omega_i,z,\Theta)),\ i=1,\cdots N_\omega\} \tag{7.c}$$

$$\mathbf{X}(\xi) = \{X(\omega_i,\xi),\ i=1,...,N_\omega\} \tag{7.d}$$

Note that $\mathbf{P}(z,\Theta)$, $\mathbf{X}(\xi)$ are complex valued vectors and that $\mathbf{G}(z,\Theta)$ is the complex transmittance matrix from the source to the receiver at position z.

Multi-source/multi-receiver discrete model

In a similar fashion one can derive (see Appendix) the multi-receiver/multi-source discrete model. The equation has the same form as above. For a tool with N_r receivers, N_s sources and N_ω sampling points in frequency domain, Equation (7a) can be generalized into the form

$$\mathbf{P}(\Theta) = \mathbf{G}(\Theta) \cdot \mathbf{X} \tag{8}$$

where $\mathbf{P}$ is an $(N \times 1)$ complex vector, with $N = N_\omega \cdot N_s \cdot N_r$; Θ is a vector of borehole/formation parameters; $\mathbf{G}$ is a $N \times M$ matrix where $M = N_\omega \cdot N_s$ with the structure shown in Figure 4; and $\mathbf{X}$ is a $M \times 1$ source array vector. The details are given in the Appendix.

NUMERICAL EXAMPLES

The case where the source characteristics are perfectly known will now be studied on synthetic data. The purpose of this exercise is to find out if the problem as defined above is properly formulated and study its conditioning. In addition it brings information about the sensitivity of the functional being minimized with respect to the parameter being inverted in a controllable manner.

The synthetic waveforms have been generated with the following formation parameters: V_p = 4 km/s, V_s = 2 km/s, V_f = 1.5 km/s, ρ_b (bulk density) = 2.3

gm/cm^3, ρ_f = 1.2 gm/cm^3, Q_p = 60, Q_s = 60, Q_f = 20, and the radius is 0.10 m. We used a Kelly source (Toksöz et al., 1983) with a center frequency ω_0 = 10 kHz.

Figures 6 to 12 show the shape of the residual energy as a function of various formation and borehole parameters. In each of the figures, we have kept all but one parameter constant. We vary that parameter about the actual model and compute the square of the difference in the pressure function (in the frequency domain) between the varied and actual models.

Figures 6 and 7 point out the fact that the determination of V_p is not as well conditioned as the determination of V_s. The shape of the residual energy function (the "incoherence") is much flatter for V_p than for V_s. This is due in part to the small P-wave energy in the signal. Furthermore, as pointed out by Cheng et al. (1982), there is very little P-wave energy in the guided wave packet, which is usually the dominant arrival in a microseismogram. The P-wave velocity is nevertheless determined by the whole waveform, rather than the mere arrival time. It can be shown that this increases the achievable signal-to-noise ratio compared with any other inversion method which does not use the complete waveform. The formation shear wave velocity, on the other hand, is very well resolved. A small error in the estimation of the shear wave velocity results in a large residual energy. Since a least squares inversion minimizes the residual energy, the formation shear wave velocity is very well constrained.

In Figure 8 one sees that a good determination of the borehole fluid velocity is necessary since the shape of the residual energy-function is drastically affected by the value of the fluid velocity. Note the same kind of behavior is observed for the variation of the energy norm as a function of the borehole radius (Figure 10). It appears therefore useful to include the caliper and independent measurements of the borehole fluid P-wave velocity as a priori in the inversion with an appropriate error covariance to take into account this inherent sensitivity.

Figure 11 illustrates the poor resolution of the density parameter ρ_b. The scale has to be magnified two orders of magnitude to see the variations as a function of ρ_b. This suggests that formation density is not well resolved in the inversion as it is set up at the present time. However, by using an external source of density measurement as a constraint to the problem, we may improve the resolution of the formation density..

In Figure 9 variations in the residual energy as a function of the P-wave quality factor Q_p are plotted. Q_p influences the function in an asymmetrical manner, and the minimum is not as sharp as for the other parameters. This suggests a reparameterization of the inversion. Instead of using Q_p as the variable, $1/Q_p$ would give the problem a better conditioning and avoid the sharp angular features in the residual energy. Physically this makes much more sense since $1/Q$ is a direct measure of attenuation (amplitude decay). The variations as a function of the P-wave attenuation are representative of the variations for all the 3 attenuation parameters.

In Figure 12 the sensitivity to the source center frequency is plotted. One can see that the source parameters do affect the waveform quite drastically and that it is a potential problem since there is plenty of experimental and theoretical evidence of the variability of the source as a function of environmental conditions. The best

solution would be to measure the source and constrain the problem with that measurement, or to use the Separable Inversion method to circumvent the source inversion problem.

Figure 13 and following illustrate the inversion of synthetic data for 4 parameters: formation P- and S-wave velocity, P-wave velocity in the borehole fluid, and formation density. Figure 13 shows the residual energy function or incoherence as a function of the number of iterations. We can see that the incoherence decreases monotonically as a function of the number of iterations. Note that V_s and V_f are much better behaved during the inversion than V_p and ρ_b (Figure 14). This illustrates the fact that the introduction of the density and the P-wave velocity creates large excursions in the parameter space. These non-physical excursions do slow down the inversion problem and can cause divergence in the case of large residuals. Again the behavior for the synthetic case suggests the limitations of the tool in real situations, and the use of additional sources of information to "robustify" the problem. One can expect therefore, without any additional a priori knowledge, that there will be comparatively large uncertainties on some of the ML answers. The MAP criterion will have to be used in the real world to obtain more reliable information about the shear velocity and attenuation.

The evolution of the synthetic full waveform that would be generated from the successive values of the 4-parameter vector and their spectra is shown in the last two figures (Figures 15 and 16). One can see the significant changes in the microseismograms and their associated spectra as the parameters converge to the model solution. Note that even between the last two iterations (7 and 11) there is a substantial change in the waveform character despite the small changes in the parameters (Figure 14).

SUMMARY

In this paper we have formulated the full waveform inversion problem for a simple cylindrical borehole. The problem is formulated in the frequency-depth domain. We demonstrated our algorithm using synthetic data in a simple one source - one receiver model. The sensitivity and the shape of the residual energy function are studied. The problem is well behaved. It is shown that formation shear wave velocity has the most influence on the residual energy function, while the formation compressional wave velocity and formation density have less influence. This information is valuable for the applying of constraints in the inversion of actual field data.

ACKNOWLEDGEMENTS

This research is supported by the Full Waveform Acoustic Logging Consortium at M.I.T.

REFERENCES

Cheng, C.H., M.N. Toksöz, and M.E. Willis, 1982, Determination of in situ attenuation from full waveform acoustic logs: J. Geophys. Res., 87, 5477-5484.

Golub, G.H. and V. Pereyra, 1973, The differentiation of pseudo-inverses and nonlinear least squares problems whose variables separate: SIAM J. Numer. Anal., 40, 413-432.

Parzen, E., 1978, Discussion on histogram splines: J. R. Stat. Soc., B, 40, 1-25.

Toksöz, M.N., C.H. Cheng and M.E. Willis, 1983, Wave types in a borehole -- a review: M.I.T. Full Waveform Acoustic Logging Consortium Annual Report, 1983.

Tsang L. and D. Rader, 1979, Numerical evaluation of the transient acoustic waveform due to a point source in a fluid-filled borehole: Geophysics, 44, 1706-1720.

Willis, M.E., 1983, Seismic velocity and attenuation from full waveform acoustic logs: Ph.D. Thesis, Massachusetts Institute of Technology, Cambridge, Massachusetts.

Willis, M.E. and M.N. Toksöz, 1983, Automatic P and S velocity determination from full waveform digital acoustic logs: Geophysics, 48, 1631-1644.

Yakowitz, S.J., 1985, Nonparametric estimation, prediction and regression for Markow sequences: J. Am. Stat. Assoc., 80, 215-221.

APPENDIX

The multi-receiver forward model

For a tool with N_r receivers, the observed set of waveforms at each receiver location $z_1, z_2, \ldots, z_{N_r}$ is modelled as

$$\mathbf{W}(\omega, z_j) = G(\omega, z_j, \Theta)\ X(\omega) + N_{z_j}(\omega) \quad \{j=1, \cdots, N_r\}. \tag{A-1}$$

In matrix form the model of the pressure field for an N_r receiver tool is

$$\mathbf{P}(\Theta) = \mathbf{G}(\Theta)\ \mathbf{X}(\xi) \tag{A-2}$$

where:

$$\mathbf{P}(\Theta) = [\{P(\omega_i, z_j, \Theta),\ i=1,\ldots,N_\omega\ ;\ j=1,\ldots,N_r\}]^T$$

$$\mathbf{G}(\Theta) = [(\mathbf{G}(z_1, \Theta),\ \cdots\ \mathbf{G}(z_j, \Theta), \cdots, \mathbf{G}(z_{N_r}, \Theta)]^T$$

with

$$\mathbf{G}(z_j, \Theta) = Diag[\{G(\omega_i, z_j, \Theta),\ i=1,\ldots,N_\omega\}]$$

$$\mathbf{X}(\xi) = [\{X(\omega_i, \xi),\ i=1, \cdots, N_\omega\}]^T$$

As shown in Figure 3, the matrix approximation for N_r receivers is obtained by algebraically "stacking" N_r models, one for each source-receiver separation, z_j. The transfer matrix $\mathbf{G}(\Theta)$ is obtained by also stacking the individual transfer matrices. The vector $\mathbf{P}(\Theta)$ has length $(N_\omega \cdot N_r)$, Matrix $\mathbf{G}$ has dimensions $(N_r \times N)$ and the source vector has length N_ω.

The multi-source/multi-receiver forward model

When the tool has an array of N_s different sources represented by complex vectors $\mathbf{X}_1$, $\mathbf{X}_2$, ...$\mathbf{X}_{N_s}$ (the Fourier spectra of each source function), a new matrix approximation is obtained by stacking N_s models as follows (see also Figure 4):

For each source indexed by u the model of the pressure field for N_r receivers is

$$\mathbf{P}_u(\Theta) = \mathbf{G}_u(\Theta)\ \mathbf{X}_u(\xi_u) \quad \{u=1, \cdots, N_s\} \tag{A-3}$$

where

$$\mathbf{P}_u(\Theta) = [\{\mathbf{P}_u(\omega_i, z_j^{(u)}, \Theta)\ ,\ i=1, \cdots, N_\omega;\ j=1, \cdots N_r\}]^T$$

$$\mathbf{G}_u(\Theta) = [(\cdots, \mathbf{G}(z_j^{(u)}, \Theta), \cdots, \mathbf{G}(z_{N_r}^{(u)}, \Theta)]^T$$

with

$$\mathbf{X}_u(\xi_u) = [\{X(\omega_i,\xi_u),\ i=1,...,N_\omega\}]^T$$

and $z_j^{(u)}$ is the distance between source (u) and receiver (j).

The N_s models of equation (A-3) "see" the same Θ and can be aggregated into one equation:

$$\mathbf{P}(\Theta,\xi) = \mathbf{G}(\Theta)\ \mathbf{X}(\xi) \tag{A-4}$$

We can re-organize the equations such that at each receiver (u) the N_s waveforms are stacked. One now has the N_s equations:

$$\mathbf{P}(z_j^{(u)}) = \mathbf{G}(z_j^{(u)},\Theta)\ \mathbf{X}_u(\xi_u)\ \ \{u=1,\cdots,N_s\} \tag{A-5}$$

with the structure shown in Figure 4. This can be written in one matrix form:

$$\mathbf{P}_j(\Theta) = \mathbf{G}_j(\Theta)\ \mathbf{X}(\xi)\ \ \{j=1,\cdots,N_r\}\ \ \xi = \{(\zeta_u),u=1,\cdots,N_s\} \tag{A-6}$$

Including all the receivers amounts to stacking the matrix equations above N_r times into one equation:

$$\mathbf{P}(\Theta) = \mathbf{G}(\Theta)\ \mathbf{X}(\xi) \tag{A-7}$$

where G now has the structure shown in Figure 4. G depends on a vector parameter Θ, and on the unknown source vector X.

The separable inversion method

The function to minimize, the residual energy, is a sum of squares of functions. The frequency domain formulation reveals that the problem has more structure than the classical nonlinear least squares because the source vector X appears linearly in the functional E:

$$E(\Theta,\mathbf{X}) = ||\mathbf{W}-\mathbf{G}(\Theta)\ \mathbf{X}||^2. \tag{A-8}$$

The approach to the solution of

$$\min_{(\Theta,\mathbf{X})} E(\Theta,\mathbf{X})$$

is to modify the residual energy functional $E(\Theta,\mathbf{X})$ such that consideration of the unknown source parameter X is deferred. The variables Θ and X are separated so that in each iteration the solution for Θ is obtained first and X is obtained in ONE STEP after that.

For any fixed $\hat{\Theta}$, the problem of finding the optimal source vector X corresponding to that $\hat{\Theta}$ is a linear least squares problem. The solution is found by:

$$X = G^{+}(\hat{\Theta})W \tag{A-9}$$

where $G^{+}(\hat{\Theta})$is the pseudo-inverse of G at $\Theta = \hat{\Theta}$.

Define now a new functional $E_2(\Theta)$ by

$$E_2(\Theta) = \min \| W - G(\Theta)\, G^{+}(\Theta) W \|^2 \tag{A-10}$$

One sees now that E_2 depends on Θ only and can be minimized with respect to Θ by means of a Gauss-Newton algorithm to give an optimal $\hat{\Theta}$. So, if there is no a priori knowledge, the separable method is

1) $\min_{\Theta} \| (I - G(\Theta)\ G^{+}(\Theta)) W \|^2$ gives $\hat{\Theta}$

2) $X = G^{+}(\hat{\Theta})\ W$

Golub and Pereyra (1973) had shown that this two-step method is equivalent to the direct inversion, provided $G(\Theta)$ has a constant rank around $\hat{\Theta}$. By taking advantage of this structure, one does not have to minimize the residual energy E with respect to the source parameters X and so the size of the nonlinear problem has been reduced.

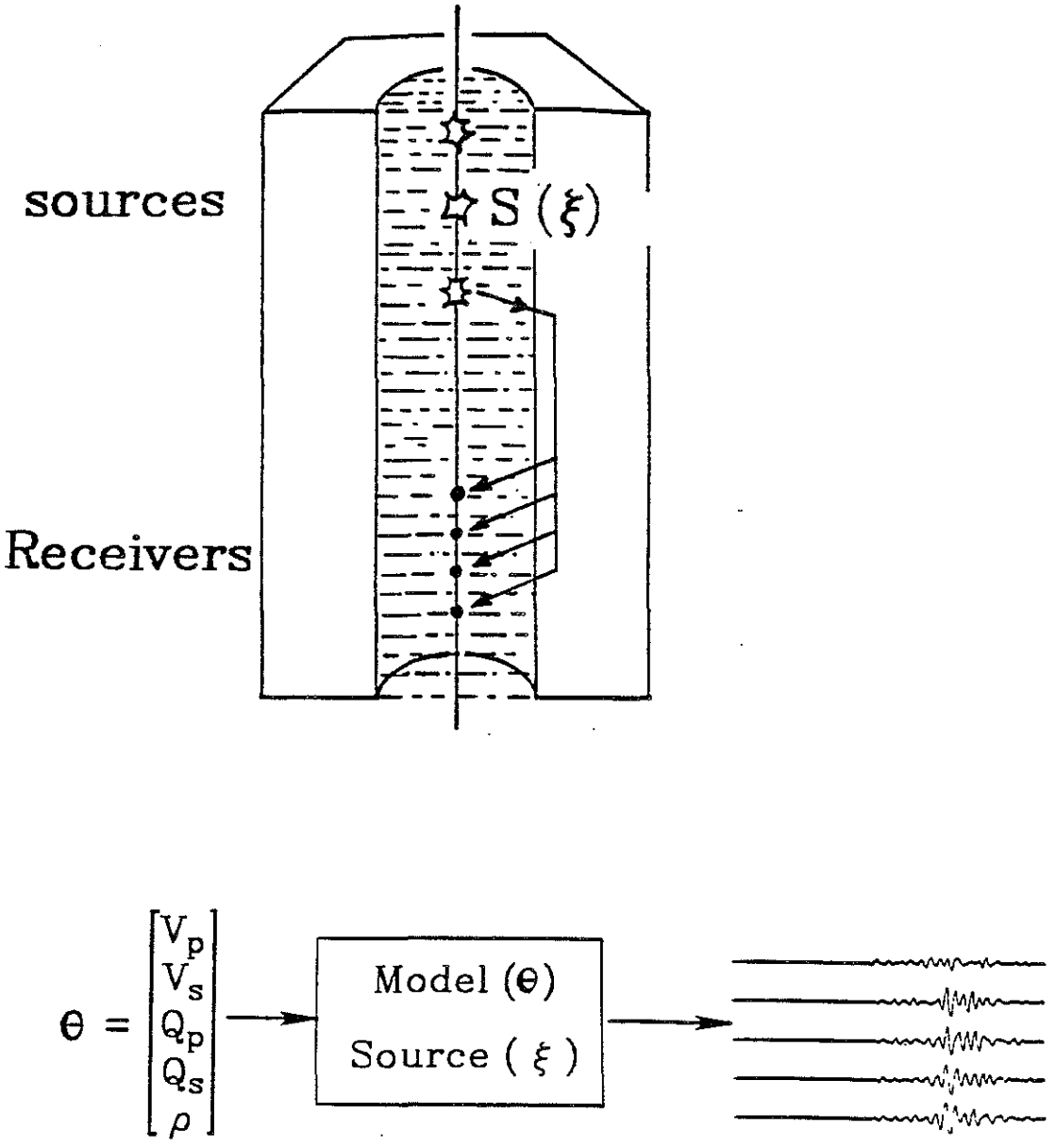

Figure 1: The Cylindrical Fluid-Filled Borehole Model.

one receiver,one source

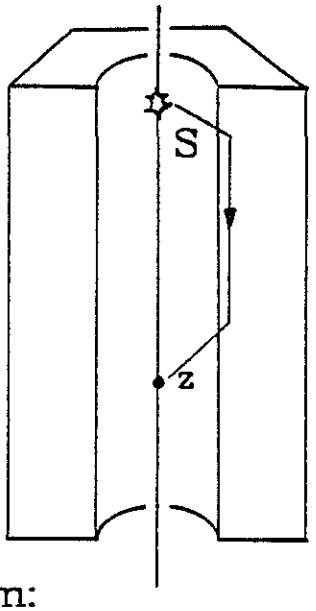

Vector-Matrix form:

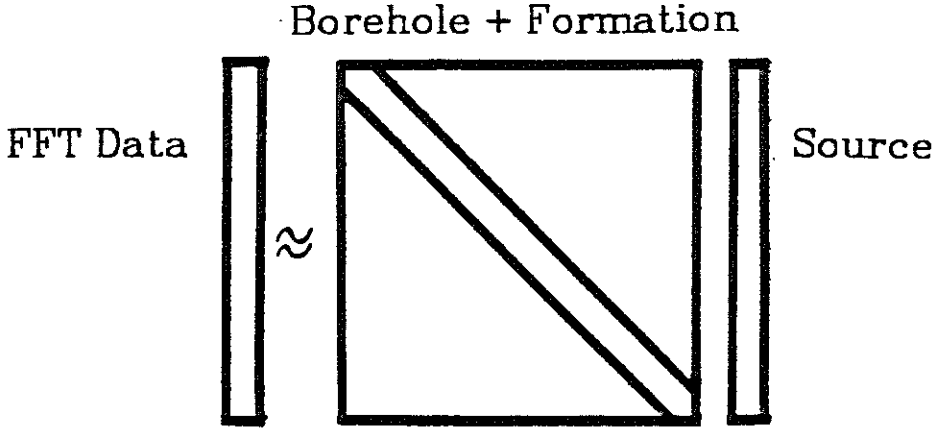

$$P_z = G_z(\theta) \cdot S(\xi) + \varepsilon$$

Figure 2: The matrix approximation structure for a one source, one receiver tool.

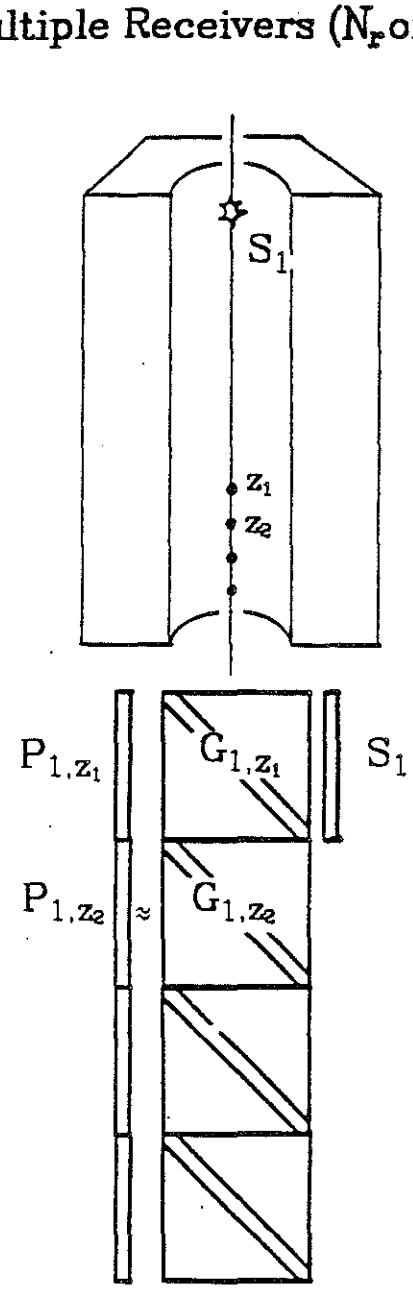

$$P = G(\theta) \cdot S(\xi) + N$$

$$N = (\varepsilon_1, \varepsilon_2, \cdots \varepsilon_N)^T$$

Figure 3: The multireceiver model.

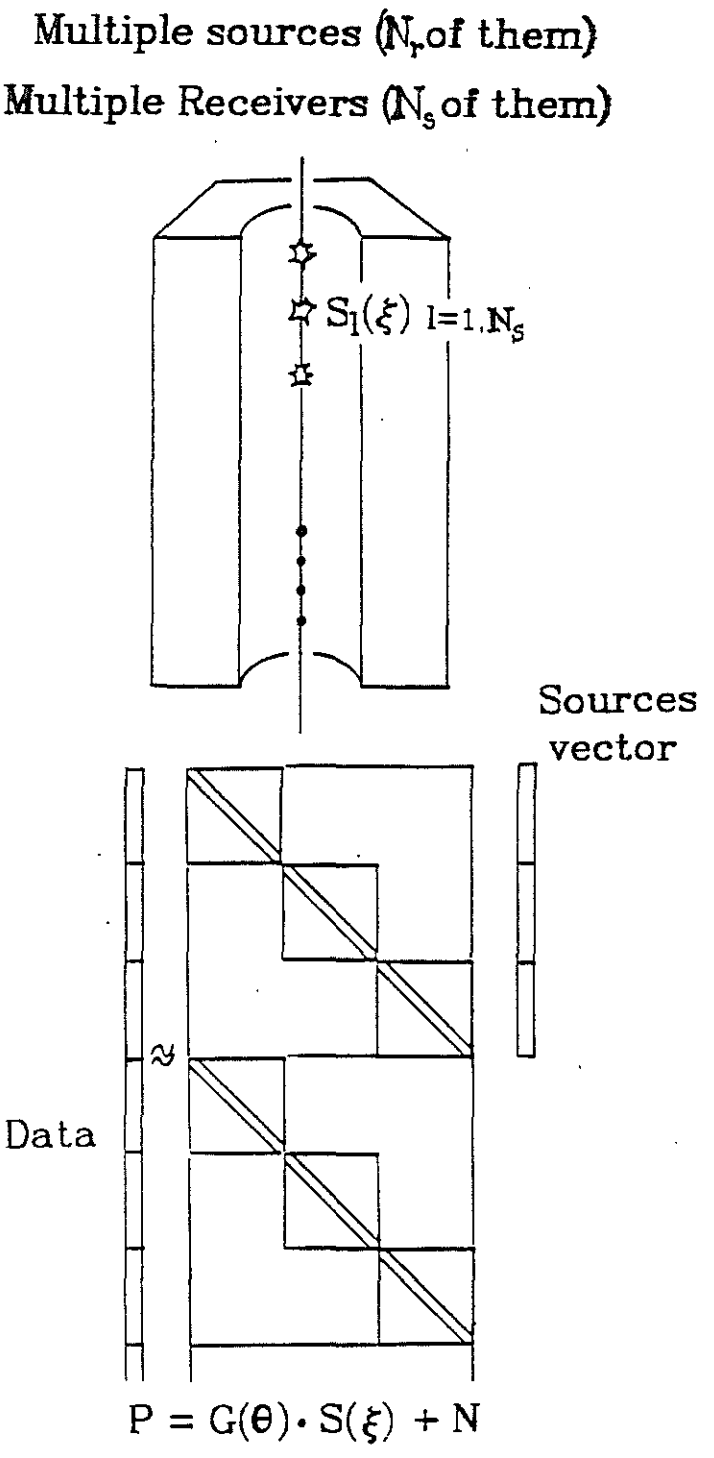

Figure 4: The multisource, multireceiver model.

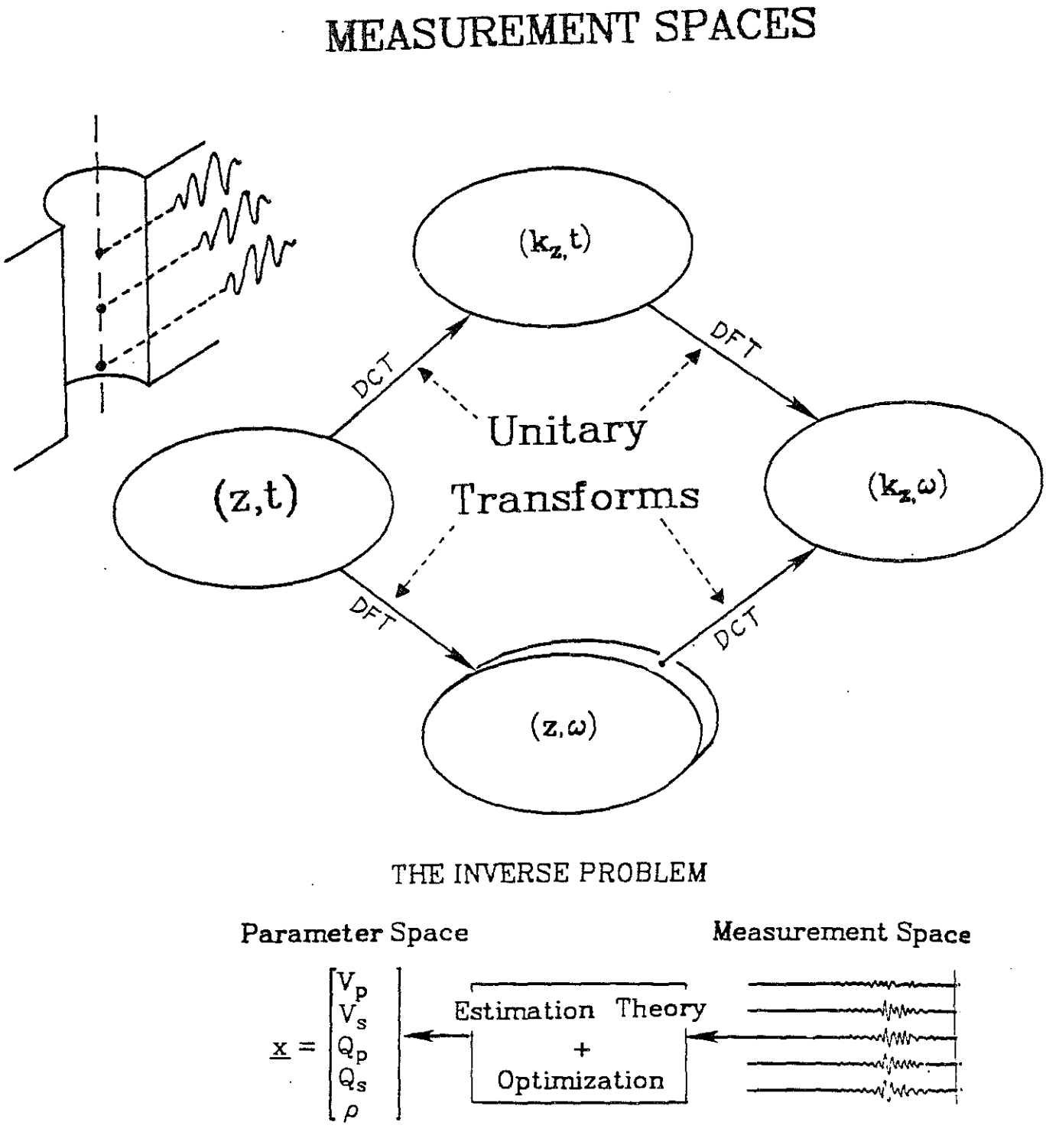

Figure 5: The unitary transform between the 4 measurement spaces.

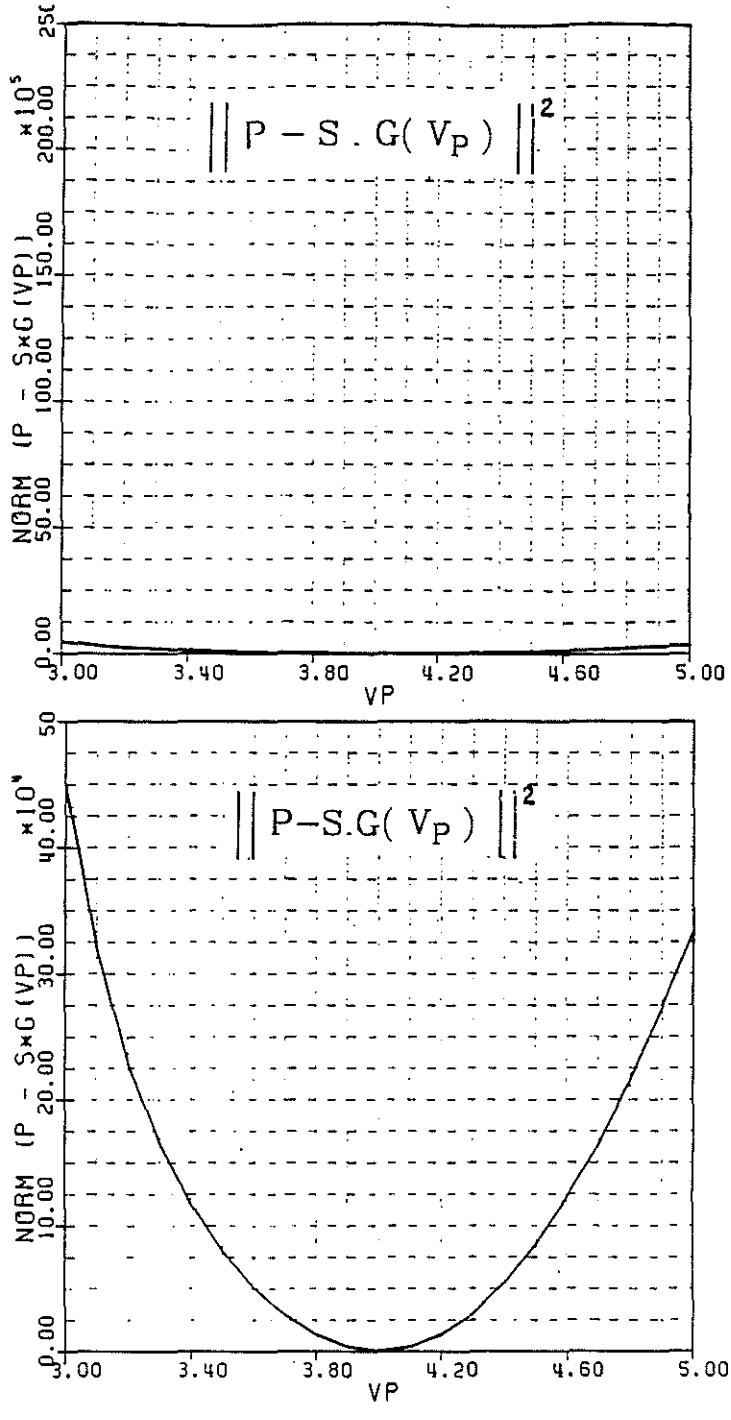

Figure 6: The one source - one receiver (1S-1R) model residual energy as a function of V_p.

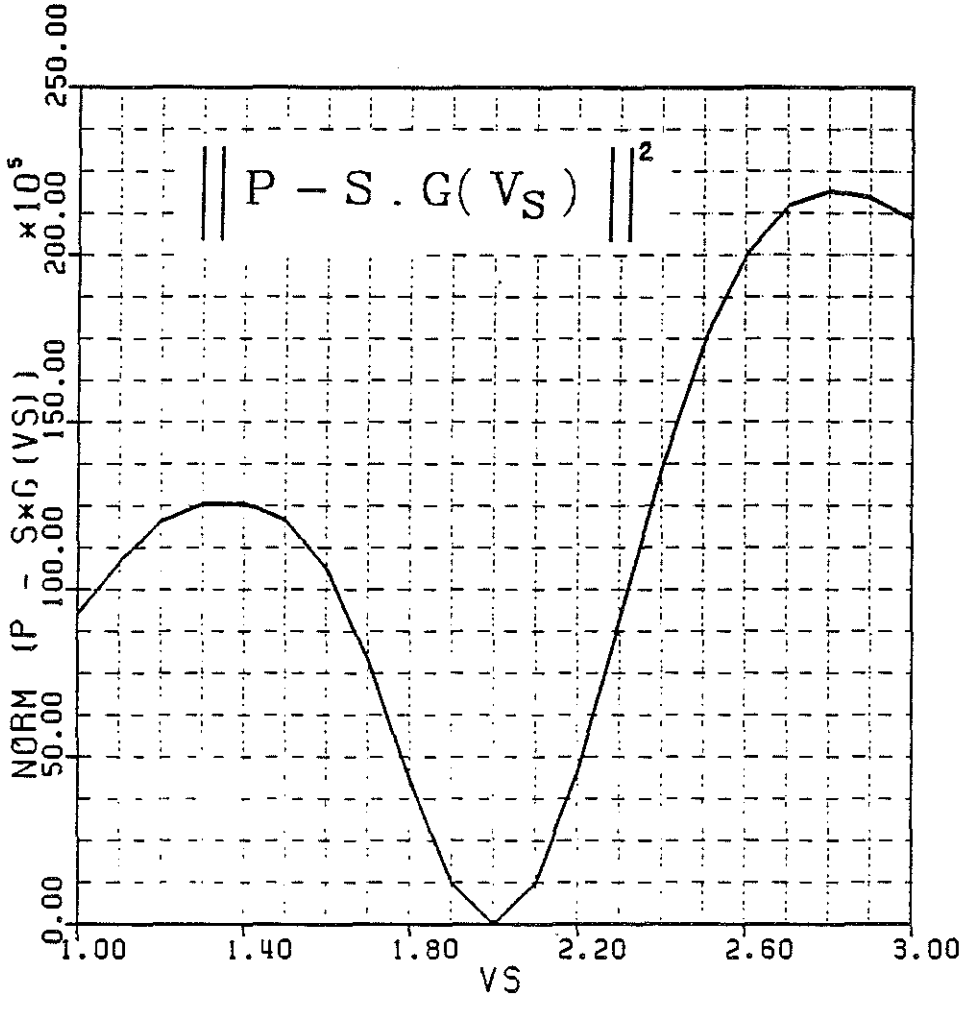

Figure 7: 1S-1R model residual energy as a function of V_s.

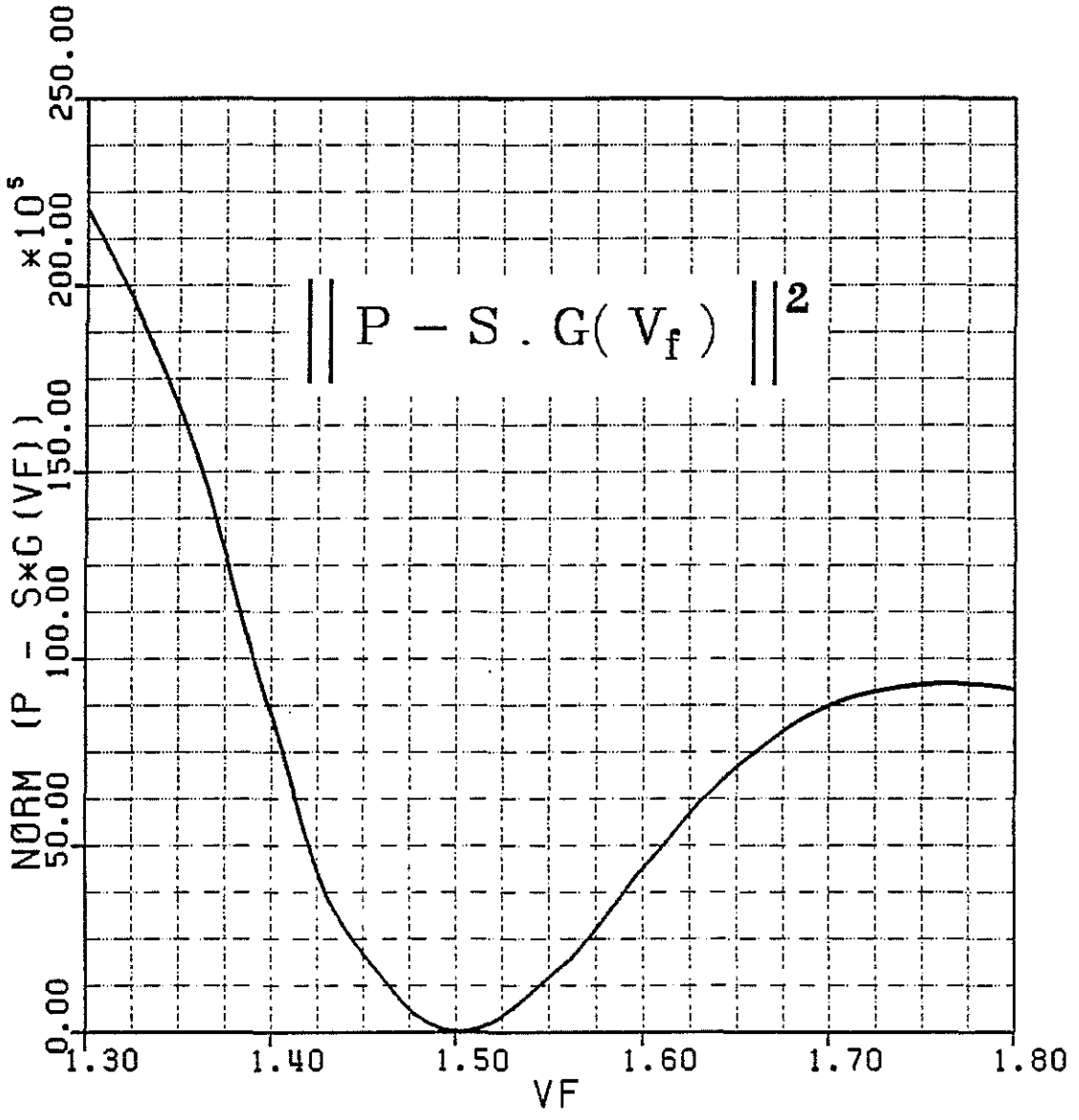

Figure 8: 1S-1R model residual energy as a function of V_f.

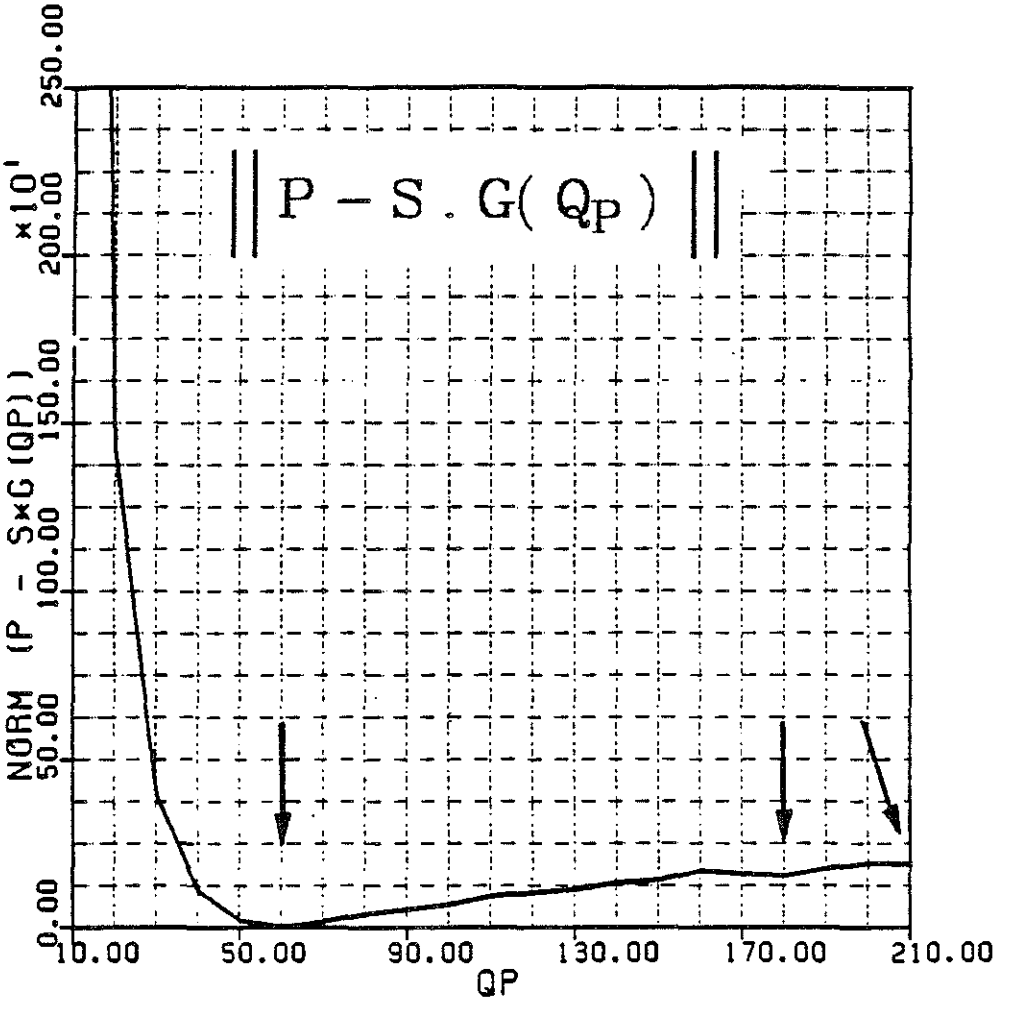

Figure 9: 1S-1R model residual energy as a function of Q_p.

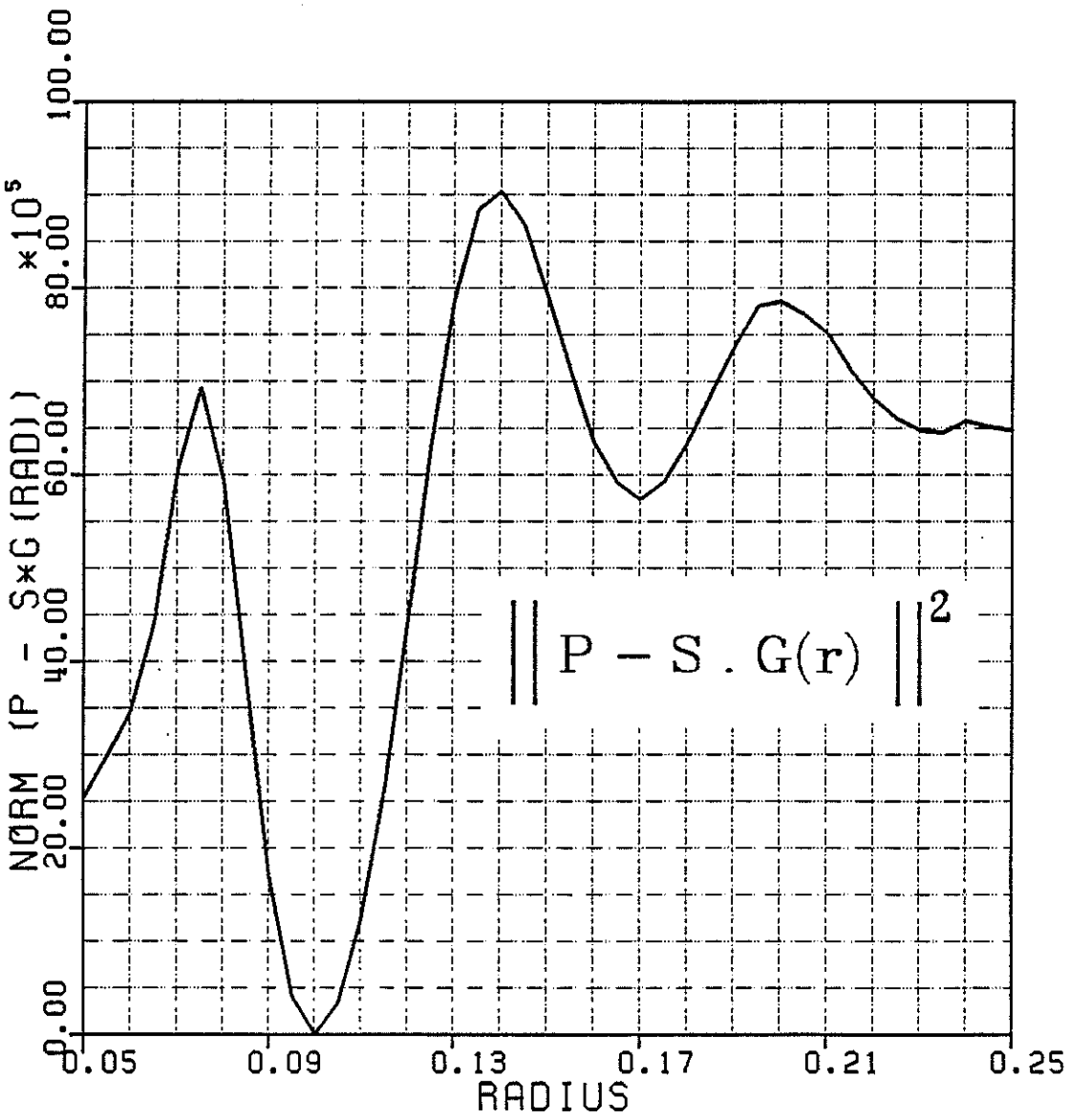

Figure 10: 1S-1R model residual energy as a function of R.

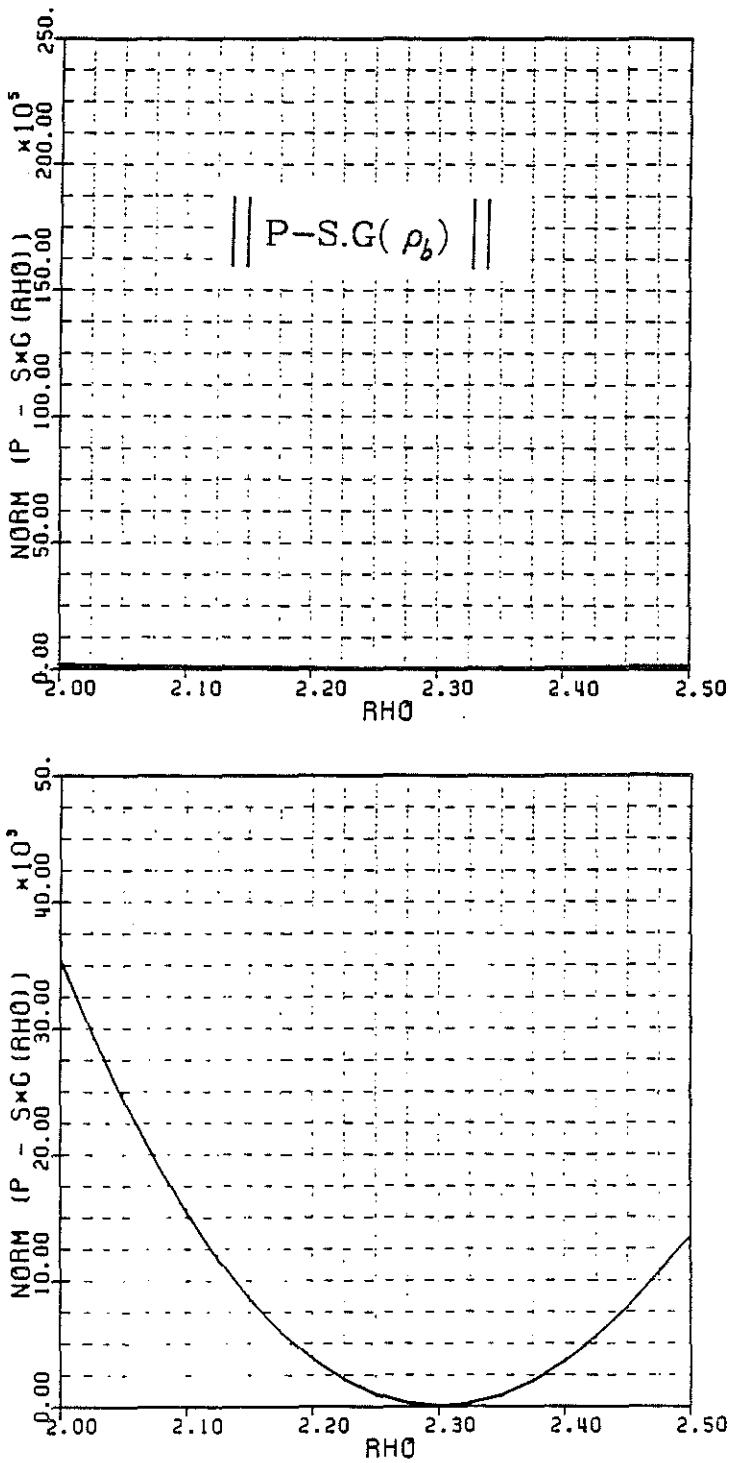

Figure 11: 1S-1R model residual energy as a function of ρ_b.

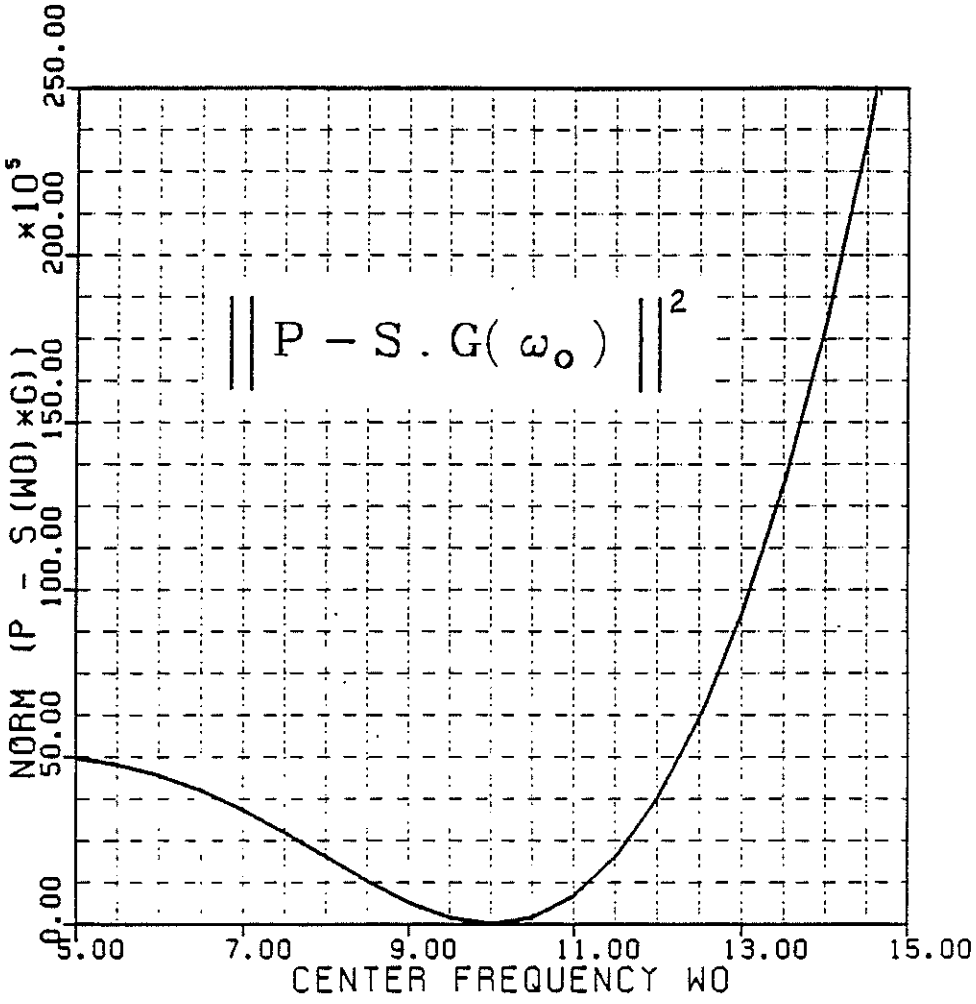

Figure 12: 1S-1R model residual energy as a function of ω_o, the source center frequency.

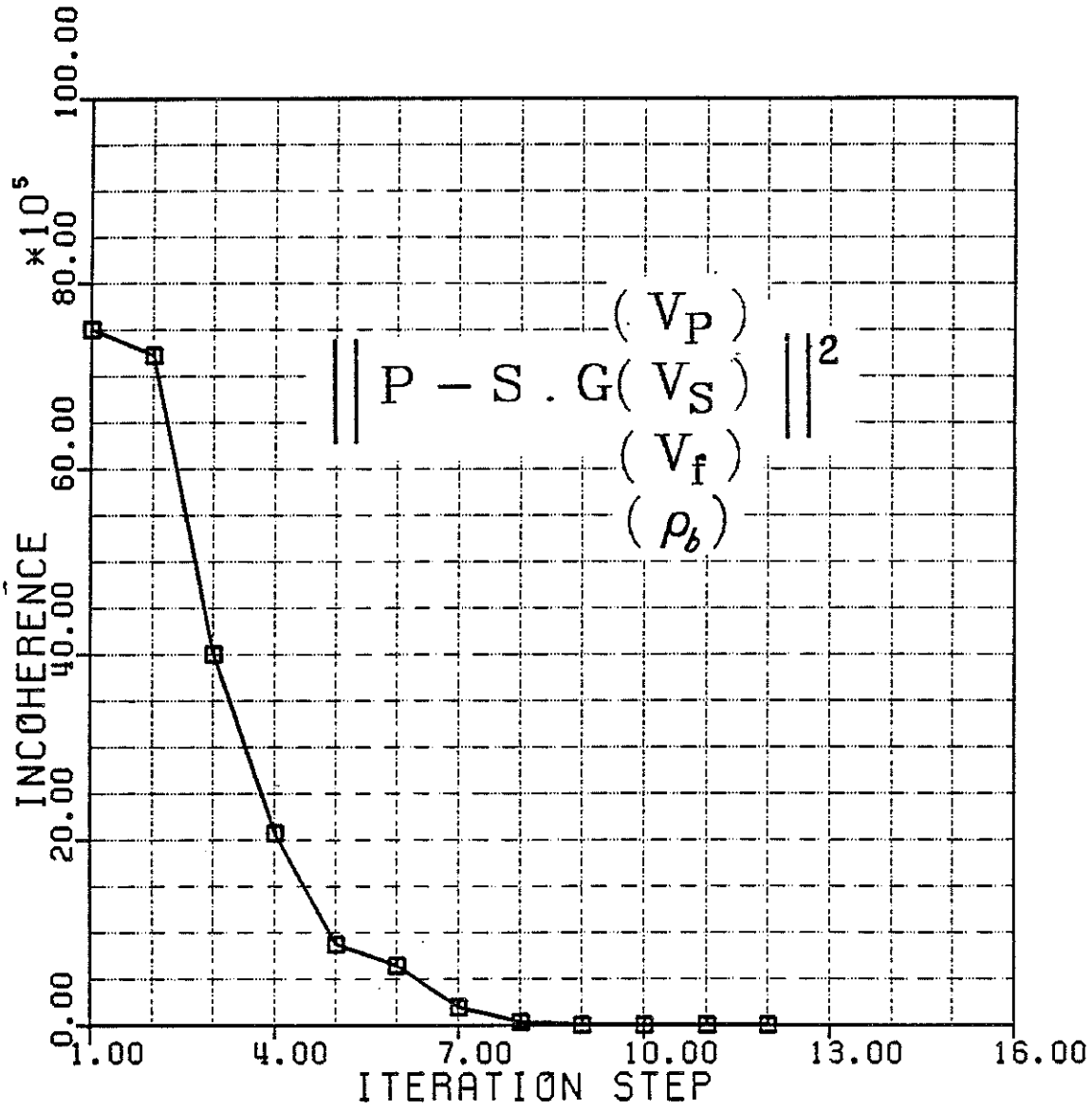

Figure 13: The residual energy reduction during a 4 parameter (V_p, V_s, V_f, ρ) inversion.

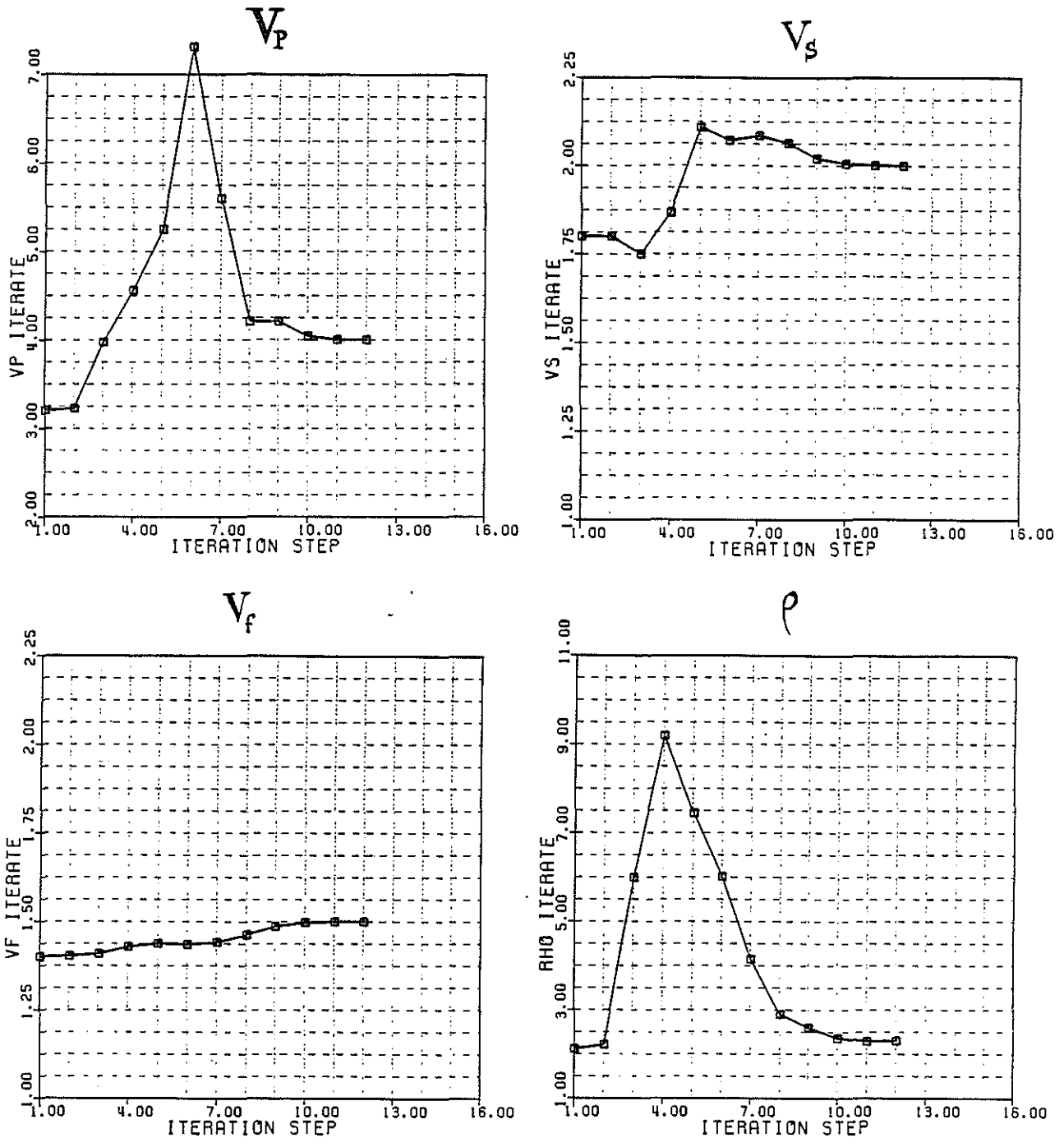

Figure 14. Residual energy reduction individual contributions (V_p, V_s, V_f, ρ).

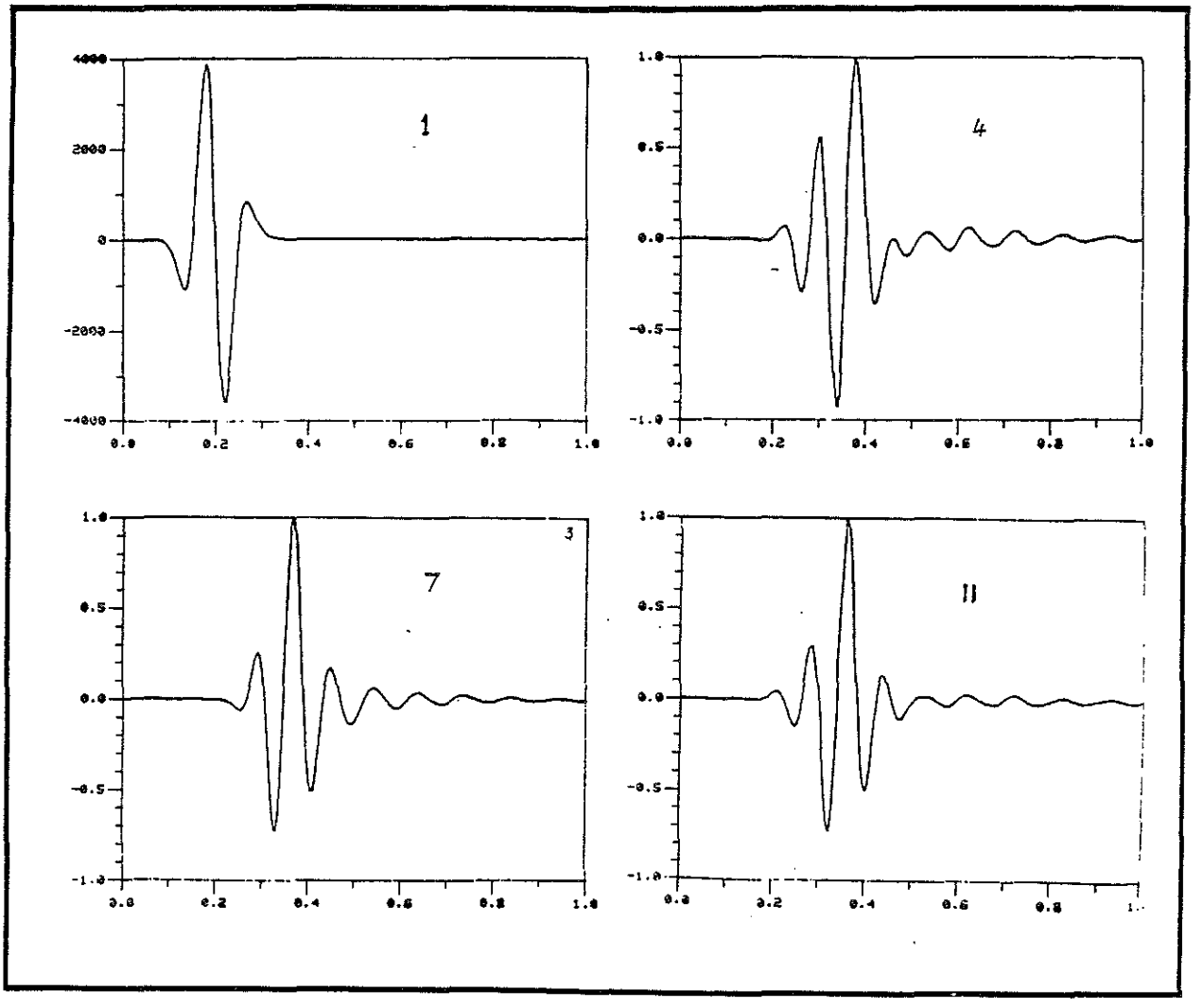

Figure 15. The time series evolution during inversion.

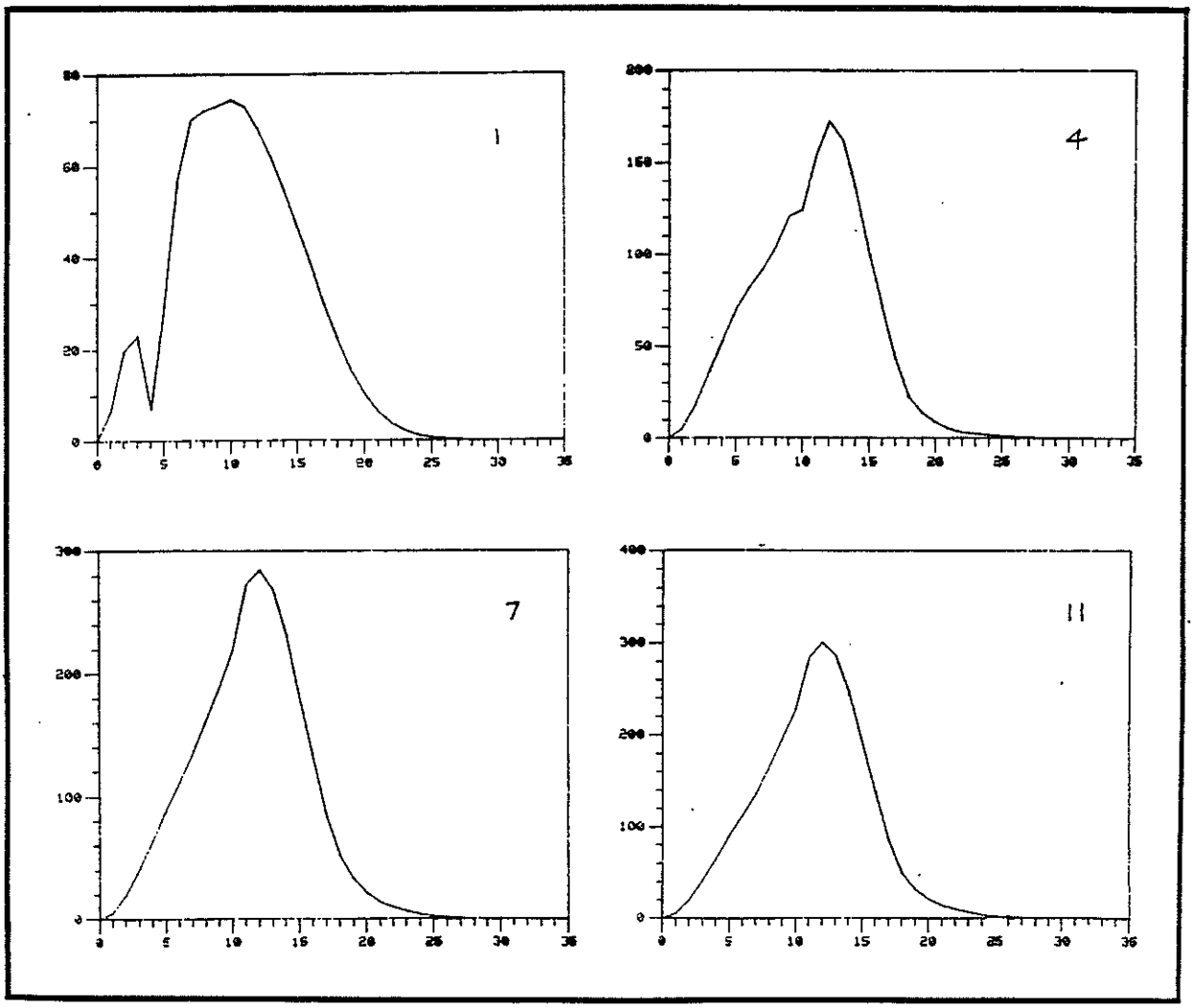

Figure 16. The spectral density evolution during inversion.